文章编号：1001－9014(2019)01－0039－05

DOI:10.11972/j.issn.1001－9014.2019.01.007

An optical design for dual-band infrared diffractive telescope

WANG Hao[1,2], KANG Fu-Zeng[1*], ZHAO Wei[1], LI Yi-Chao[1,2]

(1. State Key Laboratory of Transient Optics and Photonics, Xi'an Institute of Optics and Precision Mechanics, Chinese Academy of Sciences, Xi'an 710119, China;
2. University of Chinese Academy of Sciences, Beijing 100049, China)

Abstract: In this paper, the double-layer harmonic diffractive element (HDE) structure is investigated and the optimization procedure is based on the equation of diffraction efficiency of the double-layer diffractive optical element. The diffraction efficiency of the system in the designed middle and far infrared wavebands is larger than 99%, which improves the image contrast and the imagequality significantly. A new dual-band infrared double-layer HDE telescope is designed, which can work in the middle and far infrared wavebands. It is shown that the system approximately attains diffraction limit and is easy to processed.

Key words: diffraction efficiency, HDE, optical design
PACS: 42. 15. Eq, 07. 57. Kp

一种红外双波段衍射望远镜的光学设计

王 昊[1,2], 康福增[1*], 赵 卫[1], 李毅超[1,2]

(1. 中国科学院西安光学精密机械研究所 瞬态光学与光子技术国家重点实验室,陕西 西安 710119;
2. 中国科学院大学,北京 100049)

摘要:深入研究了双层谐衍射光学元件,基于衍射效率方程对双层衍射元件的衍射效率进行优化.光学系统在中波红外和长波红外波段的衍射效率均超过了99%,极大地提高了图像的对比度和像质.设计了一款新型的红外双波段衍射望远镜,取得了接近衍射极限的成像质量,易于加工.

关 键 词:衍射效率;HDE;光学设计

中图分类号:O439 **文献标识码**:A

Introduction

A significant improvement in reconnaissance capability is the primary goal of equipment development. It is one method to improve the equipment reconnaissance ability by using various infrared spectrum to detect the infrared radiation of the scene at the same time. Due to the influence of atmospheric transmission, radiation characteristics of different scene in the short-wavelength infrared (SWIR), medium-wavelength infrared (MWIR) and long-wavelength infrared (LWIR) have different performance. In the case of stray radiation or near the heat source, LWIR has a strong reconnaissance capability, while in hot and humid environment, MWIR has great advantage over other. It is obviously to see the difference between the image of the same scene in MWIR and LWIR[1] (Fig. 1).

By using the spectrum of different wavelength range in infrared band, the target camouflage information can be effectively eliminated, the detection and recognition ability of the target can be improved and the false alarm rate of the system can be reduced.

The refractive index of materials in the two bands varies greatly, bringing difficulty in achromatism in infrared dual band optical system. We often take a reflective structure to design dual band system to avoid the achromatic difficulty. Reflective system structure is complex that coaxial system with a central block, affects the system modulation transfer function, while off-axis system without center block is difficult to align. Refractive structures which have no center block and are easy to align

Received date: 2018-04-24, **revised date**: 2018-10-20 **收稿日期**:2018-04-24, **修回日期**:2018-10-20
Foundation items: Supported by Nationa Natural Science Foundation of China (61875227)
Biography: WANG Hao(1992-), male, Nantong, China, Ph. D. Research area involves optical design and laser propagation in undewater turbulence. E-mail: wanghao14@mails.ucas.ac.cn
* **Corresponding author**: E-mail: kangfuzeng@opt.ac.cn

take four kind materials apochromatic way to correct chromatic aberration in dual band.

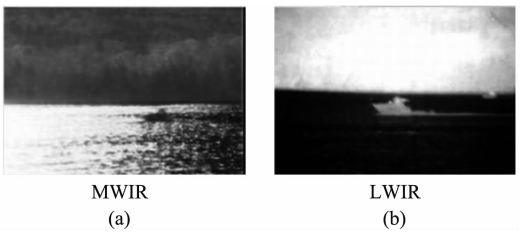

Fig. 1 The same scene in MWIR(a) and LWIR(b)
图1 在中波红外(a)和长波红外(b)的同一幅图像

The emergence of diffractive optical elements (DOEs) bring new direction to dual band optical system. Harmonic DOE can correct chromatic aberration and simplify the optical structure. Due to low diffraction efficiency of harmonic DOE, we often use double-layer HDE to design optical system.

In this paper, a dual-band infrared optical system based on Cooke structure working in both MWIR(3.4 ~ 4.2 μm) and LWIR(8 ~ 11 μm) has been designed with the double-layer HDE. In this design, the system component number and the weight of the system are reduced and the diffraction efficiency is ensured at the same time. The chromatic aberration of the system is well corrected and the image quality is near diffraction limit.

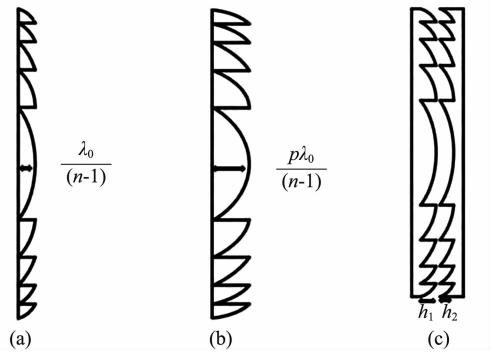

Fig. 2 Schematic diagram of different DOEs. (a) general single-layer DOE; (b) single-layer HDE; (c) double-layer HDE
图2 不同衍射元件的结构图(a)单层衍射元件(b)单层谐衍射元件(c)双层衍射元件

1 Diffraction Efficiency

Diffraction efficiency is one of the most important properties of refractive-diffractive optical systems[2]. According to the scalar diffraction theory, the diffraction efficiency of the DOE is a function of the wavelength λ and the diffraction order m:

$$\eta(\lambda, m) = \mathrm{sinc}^2\left(\frac{\Phi(\lambda)}{2\pi} - m\right) \quad . \quad (1)$$

In formula, $\mathrm{sinc}x = \sin x/x$, $\Phi(\lambda)$ is phase function of DOE.

For general DOE[2], $m = 1$, the phase function is:

$$\Phi(\lambda) = \frac{2\pi\lambda_0}{\lambda} \cdot \frac{n(\lambda) - 1}{n(\lambda_0) - 1} \quad . \quad (2)$$

It is obviously to know that the diffraction efficiency of such elements can reach 100% at the design wavelength and drops rapidly away from the design wavelength, which is not suitable for the optical system with wide spectral range.

For HDE[3-4], $m = p, p \pm 1, \cdots, p \pm i$, the phase function is:

$$\Phi(\lambda) = \frac{\rho \cdot 2\pi\lambda_0}{\lambda} \cdot \frac{n(\lambda) - 1}{n(\lambda_0) - 1} \quad . \quad (3)$$

Compared with general single-layer DOE, the diffraction efficiency of the single-layer HDE decreases more rapidly away from the design wavelength when the designed wavelength is the same.

The double-layer HDE[5-6] is equivalent to a common DOE ($m = 1$) with two single-layer HDE, the phase function is:

$$\Phi(\lambda) = \frac{2\pi h_1}{\lambda}[n_1(\lambda) - 1] - \frac{2\pi h_2}{\lambda}[n_2(\lambda) - 1] \quad . \quad (4)$$

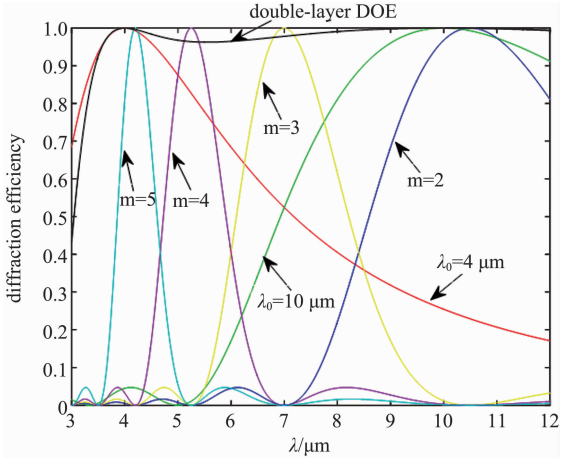

Fig. 3 Diffraction efficiency curves of general single-layer DOE, single-layer HDE and double-layer HDE (Red line and green line are diffraction efficiency curves of single-layer DOE of diffraction order $m = 1$ and designed wavelength $\lambda_0 = 4$ μm and 10 μm, respectively. Blue line, yellow line, pink line and bright blue line are diffraction efficiency curves of single-layer HDE of $p = 3$ and designed wavelength $\lambda_0 = 7$ μm, which's diffraction order m is 2, 3, 4 and 5, respectively. Black line is diffraction efficiency curve of double-layer HDE of diffraction order m = 1 and designed wavelength $\lambda_1 = 4$ μm and $\lambda_2 = 10$ μm)
图3 不同衍射元件的衍射效率曲线(红线和绿线是衍射级次 $m = 1$,设计波长 λ_0 分别选择4 μm 和10 μm 的单层衍射元件的衍射曲线;蓝线、黄线、粉红线和亮蓝线是 $p = 3$,设计波长 $\lambda_0 = 7$ μm,衍射级次分别为2、3、4、5 的单层谐衍射元件的衍射曲线;黑线是衍射级次 $m = 1$,设计波长 λ_1 和 λ_2 选择4 μm 和10 μm 的双层谐衍射元件的衍射曲线)

From figure 3, we can see that diffraction efficiency of double-layer HDE is much higher than that of single-layer DOE and single-layer HDE and associated with design wavelengths. After selecting two different dispersive materials and λ_1 and λ_2, the two design wavelengths in the dual-design wavebands, we can obtain the following

relation[6]:

$$\begin{aligned}[n_1(\lambda_1)-1]H_1+[n_2(\lambda_1)-1]H_2&=m\lambda_1\\ [n_1(\lambda_2)-1]H_1+[n_2(\lambda_2)-1]H_2&=m\lambda_2\end{aligned}. \quad (5)$$

By solving Eq. (5), the surface relief heights of the two HDE for the corresponding design wavelengths are

$$H_1=\frac{m\lambda_1(n_2(\lambda_2)-1)-m\lambda_2(n_1(\lambda_1)-1)}{(n_1(\lambda_1)-1)(n_2(\lambda_2)-1)-(n_1(\lambda_2)-1)(n_2(\lambda_1)-1)}$$

$$H_2=\frac{m\lambda_1(n_1(\lambda_2)-1)-m\lambda_2(n_1(\lambda_1)-1)}{(n_1(\lambda_1)-1)(n_2(\lambda_2)-1)-(n_1(\lambda_2)-1)(n_2(\lambda_1)-1)}. \quad (6)$$

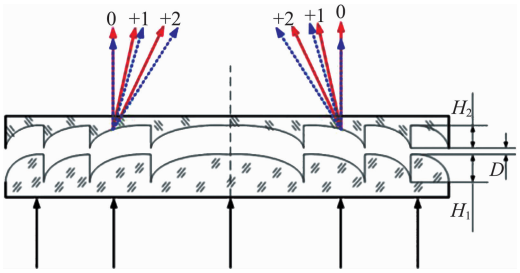

Fig. 4 (Color online) Structure of double-layer HDE. H_1 and H_2 are respectively the surface relief heights of the first and second HDE. D is the width of the air gap. The solid and dashed lines are the diffractive directions for MWIR and LWIR, respectively

图 4　双层衍射元件的结构图. H_1 和 H_2 分别为第一层和第二层衍射元件的高度,D 是空气间隔. 实线和虚线分别为中波红外和长波红外的衍射方向

Then the value of the comprehensive average diffraction efficiency (CADE)[6] for dual wavebands can be written as:

$$\bar{\eta}=\frac{w_1}{\lambda_{1\max}-\lambda_{1\min}}\int_{\lambda_{1\min}}^{\lambda_{1\max}}\mathrm{sinc}^2\left(\frac{\Phi(\lambda)}{2\pi}-m\right)\mathrm{d}\lambda+\frac{w_2}{\lambda_{2\max}-\lambda_{2\min}}\int_{\lambda_{2\min}}^{\lambda_{2\max}}\mathrm{sinc}^2\left(\frac{\Phi(\lambda)}{2\pi}-m\right)\mathrm{d}\lambda, \quad (7)$$

where $\lambda_{1\min}$ and $\lambda_{1\max}$ and $\lambda_{2\min}$ and $\lambda_{2\max}$ are respectively the minimum and maximum wavelength for the two wavebands, and w_1 and w_2 are the weight factors of CADE for each waveband. Because the imaging quality of the hybrid diffractive-refractive optical system is analyzed alone for each waveband, w_1 and w_2 are 0.5.

In the paper, we choose ZnSe and SRF2 as the first and second base material of double-layer HDE for different design wavelength pairs. According to Eq. (7), we use Matlab to find the best chose wavelength pairs for the highest diffraction efficiency. From the Fig. 5 and Fig. 6, we can see that when $\lambda_1=3.852$ μm and $\lambda_2=9.485$ μm, the CADE can reach 99.84%. At the same time, $H_1=22.927$ μm, $H_2=59.507$ μm and $m_1=7.4$, $m_2=-6.4$.

2 Design of the infrared double-layer diffractive telescope

The dual-band infrared double-layer HDE telescope optical system[7-10] with four different materials and four

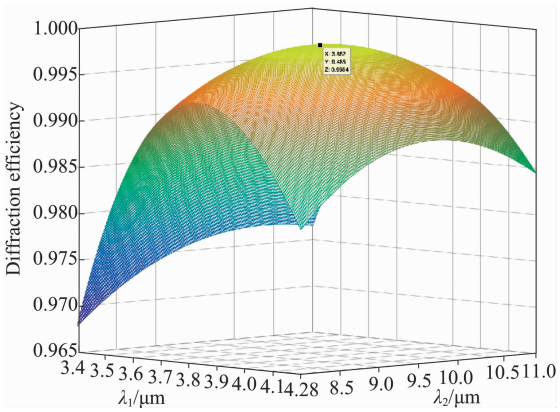

Fig. 5 Diffraction efficiency of double-layer HDE under different wave pair (front view)

图 5　不同波长对下的双层衍射元件的平均衍射效率

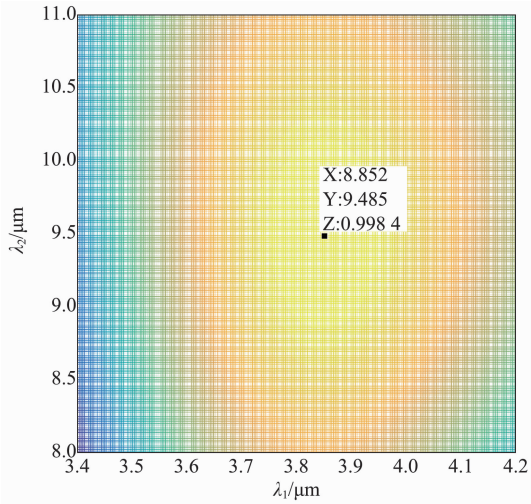

Fig. 6 Diffraction efficiency of double-layer HDE under different wave pair (top view)

图 6　不同波长对下的双层衍射元件的平均衍射效率（俯视）

Table 1 CADE of double-layer HDE with Different Design Wavelength Pairs

表 1　双层衍射元件在不同的设计波长对下面的平均衍射效率

Design wavelength / μm	3.852 and 9.485	3.2 and 8	3.8 and 10.5	4.2 and 11
CADE/%	99.84	96.79	98.92	98.44

lenses must satisfy the three relations as follows:

the total power:

$$\Phi_1^1+\Phi_1^2+\Phi_1^3+\Phi_1^4+\Phi_{1d}^5=\Phi, \quad (8)$$

zero axial color over the two wavebands:

$$\frac{\Phi_1^1}{v_1^1}+\frac{\Phi_1^2}{v_1^2}+\frac{\Phi_1^3}{v_1^3}+\frac{\Phi_1^4}{v_1^4}+\frac{\Phi_{1d}^5}{v_{1d}^5}, \quad (9)$$

$$\frac{\Phi_2^1}{v_2^1}+\frac{\Phi_2^2}{v_2^2}+\frac{\Phi_2^3}{v_2^3}+\frac{\Phi_2^4}{v_2^4}+\frac{\Phi_{2d}^5}{v_{2d}^5}, \quad (10)$$

where Φ_1^1, Φ_1^2, Φ_1^4 and Φ_1^4 are the respective powers of the three refractive lens in the mid-infrared waveband and

Φ_{1d}^5 is that of the HDE. v_1^1, v_1^2, v_1^3 *and* v_1^4 are the respective dispersion coefficients for the materials of the lens and V_{1d}^5 is that of the HDE. $\Phi_2^i, v_2^i, (i=1,2,3,4)$ and Φ_{2d}^5, v_{2d}^5 are the corresponding quantities over the far-infrared waveband.

Based on the discussion, we can select the four materials as follows: ZnS, Ge, ZnSe and SRF2. And the optical system uses Selex Company's MW/LW CCD infrared detector(HxV is 640×512, Pixel Pitch is 30 μm ×30 μm). The optical specifications of the optical system are summarized in Table 2.

Table 2 Design specifications
表 2 设计参数

Waveband	3.4 ~ 4.2 μm and 8 ~ 11 μm
Focal length	50 mm
F number	2
Field of view	16°
MTF	Above 0.5 at 17 pl/mm

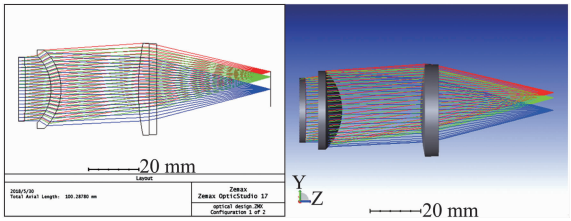

Fig. 7 Structure of the infrared double-layer HDE telescope optical system
图 7 红外双波段衍射望远镜的结构图

In figure 7, the surface 1 is aspheric surface which well corrects spherical aberration and improves the image quality of system. The achromatic surface 6 and surface 7 are binary optical surfaces.

In figure 8, the maximum RMS radius in 3.4 ~ 4.2 μm and 8 ~ 11 μm are10.279 μm and 15.327 μm, respectively, which means that the lens can match with the infrared CCD detector that has a format of 640×512 and a pixel pitch of 30 μm.

The curve of the modulation transfer function (MTF) in mid- and far-infrared wavebands are shown in Fig 9. At the spatial frequency of 17 lp/mm, the MTF at the center FOV(0°) in dual wavebands attained above

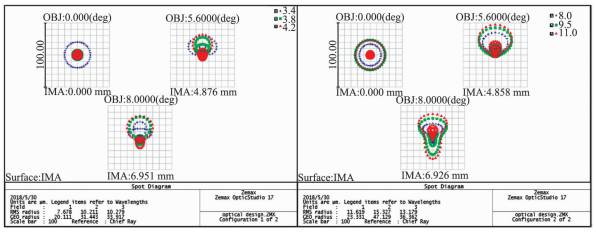

Fig. 8 Spot diagram of the infrared double-layer HED telescope. Left: spot diagram of the optical system in the mid-infrared waveband; right: spot diagram of the optical system in the far-infrared waveband
图 8 红外双波段衍射望远镜在中波红外(左边)和长波红外(右边)波段的点列图

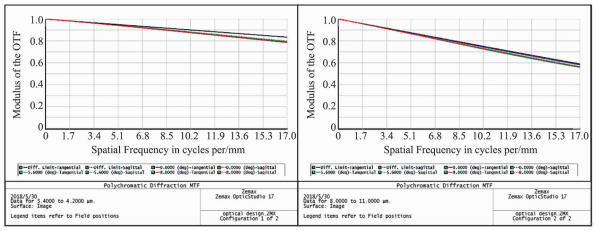

Fig. 9 MTF of the infrared double-layer HDE telescope optical system. Left: MTF of the optical system in the mid-infrared waveband; right: MTF of the optical system in the far-infrared waveband
图 9 红外双波段衍射望远镜在中波红外(左边)和长波红外(右边)波段的 MTF

0.57 and that of edge FOV(8°) in 3.4 ~ 4.2 μm and 8 ~ 11 μm attained 0.78 and 0.56, respectively. The diffraction efficiency of the system at each wavelength in the two designed wavebands is larger than 99%, which improves the image contrast and the imaging quality significantly.

In figure 10, we can easy find that the feature size of surface 6 is 29.6 μm and that of surface 7 is 30.9 μm. Under existing level of manufacture, Diamond Turning can meet the requirement of manufacture.

3 Conclusion

In conclusion, the optimization structure of the double-layer HDE is investigated in order to conquer the difficulty of the diffraction efficiency of the single layer

Table 3 Structural parameters of infrared double-layer HDE optical system (unit: mm)
表 3 红外双波段衍射望远镜的结构参数(单位:mm)

	Surface	Radius	Thickness	Glass	Semi-diameter
OBJ	Standard	Infinity	Infinity		Infinity
STO	Even asphere	-3 637.459	2.632	ZnS	12.447
2	Standard	-335.167	10.215		12.636
3	Standard	-18.699	4	Germanium	13.247
4	Standard	-21.516	30.798		15.431
5	Standard	91.855	4.264	ZnSe	18.205
6	Binary 2	Infinity	0		17.989
7	Binary 2	Infinity	3	SRF2	17.989
8	Standard	7 366.987	45.637		17.454
IMA	Standard	Infinity	—		6.963

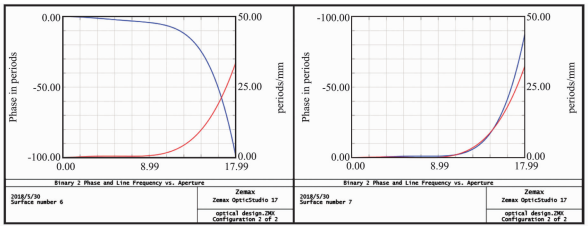

Fig. 10　Phase plot of binary surface. Left: phase plot of the optical system in the mid-infrared waveband; right: phase plot of the optical system in the far-infrared waveband

图 10　二元面在中波红外(左边)和长波红外(右边)波段的相位分布图

HDE, and the optimization method is investigated. Then an infrared telescope with a double-layer HDE is designed. Its diffraction efficiency is larger than 99% at each wavelength in the mid and far-infrared wavebands, which improves the image contrast and the image performance significantly. MTF is above 0.5 at 17 lp/mm and image performance is near-diffraction. And it is applicable to the uncooled infrared dual waveband CCD detector that has a format of 640 × 512 which's pixel pitch is 30 μm. By introducing double-layer HDE in optical design, chromatic aberration is well corrected.

References

[1] Hinnrichs M. Dual band (MWIR/LWIR) hyperspectral imager, in: 32nd [C], *Applied Imagery Pattern Recognition Workshop*, 2003, **3**: 73 - 78.

[2] Veldkamp W B, McHugh T J. Binary optics[J]. *Scientific American*, 1992, **266**: 92 - 97.

[3] Sweeney D W, Sommargren G E. Harmonic diffractive lenses[J]. *Appl Opt*, 1995, **34**: 2469 - 2475.

[4] Faklis D, Morris G M. Spectral properties of multiorder diffractive lenses[J]. *Appl Opt*, 1995, **34**: 2462 - 2468.

[5] Arieli Y. , Ozeri S. , N. Eisenberg, Design of diffractive optical elements for multiple wavelengths [J], *Opt. Lett*. 1998, **11**: 6174 - 6177.

[6] Chunyan, C. X. Xue, Q. F. Cui, J. B. Tong, Design of Multi-Layer Diffractive Optical Element with Bandwidth Integral Average Diffraction Efficiency [J], *Acta Optica Sinica*, 2010, **10**: 048.

[7] Sun Q, Lu Z W, Wang Z Q, The dual band design of harmonic diffractive/refractive optics system [J]。*Acta Opt. Sin*. 2004 , **24**: 830 - 833.

[8] Sun Q, Wang Z Q. Study of an athermal infrared dual band optical system design containing harmonic diffractive element [J]. *Chin. Sci. Bull*. 2003, **48**: 1193 - 1198.

[9] ZHANG Liang, MAO Xin, WANG He-Long. The design of MWIR/LWIR multiple FOV optical system[J] *J. Infrared Millim. Waves*, (张良, 毛鑫, 王合龙. 中波/长波双色多视场光学系统设计. 红外与毫米波学报, 2013, **32**(3): 254 - 259.

[10] Ma H T, Zhang X H, Han Bing. Design of telescope system with a wide spectrum, large field and small distortion [J]. *Infrared and Laser Engineering*. 2013, **7**: 020.

(上接第 31 页)

[8] Jongwon Yun, Namhyung Kim, Daekeun Yoon, *et al*. A 248-262 GHz InP HBT VCO with interesting tuning behavior[J]. *IEEE Microwave and Wireless Components Letters*, 2014, **24**(8), 560 - 562.

[9] Zhong Ying-Hui, Su Yong-Bo, Jin Zhi, *et al*. An InGaAs /InP W-band dynamic frequency divider[J]. *J. Infrared Millim. Waves*, (钟英辉, 苏永波, 金智, 等. W 波段 InGaAs/InP 动态二分频器. **红外与毫米波学报**) 2012, **31**(5), 393 - 398.

[10] Adar A, Ramachandran R. An HBT MMIC wideband VCO [C]. *IEEE Microwave and Millimeter-wave Circuits Symposium*, USA, MA, 1991: 73 - 76.

[11] Makon R E, Driad R, Schneider K, *et al*. Fundamental W-Band InP DHBT-Based VCOs with low phase noise and wide tuning range[C]. *IEEE MTT-S International Microwave Symposium*, USA, HI, 2007: 649 - 652.

[12] Stuenkel M, Feng M. An InP VCO with static frequency divider for millimeter wave clock generation, *IEEE Compound Semiconductor Integrated Circuit Symposium* (*CSICS*), USA, CA, 2010: 1 - 4.

[13] Thomas Jensen, Thualfiqar Al-sawaf, Marco Lisker. Millimeter-wave hetero-integrated sources in InP-on-BiCMOS technology[J]. *International Journal of Microwave and Wireless Technologies*, 2014, **6**(3/4), 225 - 233.